

## Generalized random sequential adsorption of polydisperse mixtures on a one-dimensional lattice

This article has been downloaded from IOPscience. Please scroll down to see the full text article.

J. Stat. Mech. (2010) P02022

(<http://iopscience.iop.org/1742-5468/2010/02/P02022>)

[The Table of Contents](#) and [more related content](#) is available

Download details:

IP Address: 147.91.1.44

The article was downloaded on 11/03/2010 at 09:06

Please note that [terms and conditions apply](#).

# Generalized random sequential adsorption of polydisperse mixtures on a one-dimensional lattice

I Lončarević<sup>1</sup>, Lj Budinski-Petković<sup>1</sup>, S B Vrhovac<sup>2</sup>  
and A Belić<sup>2</sup>

<sup>1</sup> Faculty of Engineering, Trg Dositeja Obradovića 6, Novi Sad 21000, Serbia

<sup>2</sup> Institute of Physics, PO Box 68, Zemun 11080, Belgrade, Serbia

E-mail: [ivanalon@uns.ac.rs](mailto:ivanalon@uns.ac.rs), [ljupka@uns.ac.rs](mailto:ljupka@uns.ac.rs), [vrhovac@ipb.ac.rs](mailto:vrhovac@ipb.ac.rs) and [abelic@ipb.ac.rs](mailto:abelic@ipb.ac.rs)

URL: <http://www.ipb.ac.rs/~vrhovac/>

Received 19 October 2009

Accepted 21 January 2010

Published 25 February 2010

Online at [stacks.iop.org/JSTAT/2010/P02022](http://stacks.iop.org/JSTAT/2010/P02022)

doi:10.1088/1742-5468/2010/02/P02022

**Abstract.** Generalized random sequential adsorption (RSA) of polydisperse mixtures of  $k$ -mers on a one-dimensional lattice is studied numerically by means of Monte Carlo simulations. The kinetics of the deposition process of mixtures is studied for the irreversible case, for adsorption–desorption processes and for the case where adsorption, desorption and diffusion are present simultaneously. We concentrate here on the influence of the number of mixture components and the length of the  $k$ -mers making up the mixture on the temporal behavior of the coverage fraction  $\theta(t)$ . The approach of the coverage  $\theta(t)$  to the jamming limit  $\theta_{\text{jam}}$  in the case of irreversible RSA is found to be exponential,  $\theta_{\text{jam}} - \theta(t) \propto \exp(-t/\sigma)$ , not only for a whole mixture, but also for the individual components. For the reversible deposition of polydisperse mixtures, we find that after the initial ‘jamming’, a stretched exponential growth of the coverage  $\theta(t)$  towards the equilibrium state value  $\theta_{\text{eq}}$  occurs, i.e.,  $\theta_{\text{eq}} - \theta(t) \propto \exp[-(t/\tau)^\beta]$ . The characteristic timescale  $\tau$  is found to decrease with the desorption probability  $P_{\text{des}}$ . When adsorption, desorption and diffusion occur simultaneously, the coverage of a mixture always reaches an equilibrium value  $\theta_{\text{eq}}$ , but there is a significant difference in temporal evolution between the coverage with diffusion and that without.

**Keywords:** surface diffusion (theory), thin film deposition (theory), stochastic processes (theory)

---

**Contents**

<b>1. Introduction</b>	<b>2</b>
<b>2. Random sequential adsorption of polydisperse mixtures</b>	<b>3</b>
<b>3. Adsorption, desorption and diffusion of mixtures</b>	<b>8</b>
<b>4. Concluding remarks</b>	<b>15</b>
<b>Acknowledgments</b>	<b>18</b>
<b>References</b>	<b>18</b>

---

**1. Introduction**

Adsorption of large molecules on solid surfaces is often irreversible over experimental timescales and can be studied using the random sequential adsorption (RSA) model [1]–[5]. In RSA processes particles are randomly, sequentially and irreversibly deposited onto a substrate. The particles are not allowed to overlap and there is no diffusion of the adsorbed particles. The dominant effect in RSA is the blocking of the available substrate area. Within a monolayer deposit, each adsorbed particle affects the geometry of all later placements. When the surface is saturated with the adsorbed objects and no further objects can be placed, the system reaches the jamming limit  $\theta_{\text{jam}}$ . The kinetic properties of a deposition process are described through the time evolution of the coverage  $\theta(t)$ , which is the fraction of the substrate area occupied by the adsorbed particles. For lattice RSA models the approach to the jamming coverage is exponential [6]–[9]:

$$\theta(t) = \theta_{\text{jam}} - Ae^{-t/\sigma}, \quad (1.1)$$

where  $A$  and  $\sigma$  are parameters that depend on the details of the model, such as the shape and orientational freedom of the depositing objects.

However, modeling real physical situations, one often needs to take into account the possibility of desorption or diffusion of deposited particles [10]–[12]. Generalized random sequential adsorption includes these desorption and diffusion processes. Problems including adsorption and desorption of particles along a one-dimensional track are related to many biophysical processes. Binding and unbinding of kinesin motors to microtubules [13], of myosin to actin filaments, and of proteins to DNA are commonly studied biological examples. The adsorption–desorption processes can also reproduce many experimentally observed phenomena in granular materials, such as density relaxation in vibrated granular materials [11], [14]–[17] and memory effects [12, 18].

Allowing desorption makes the process reversible and the system ultimately reaches an equilibrium state. The density of the particles in the equilibrium state is a function only of the desorption to adsorption rate ratio [19, 20]. The approach of the coverage to its equilibrium value was found to be exponential for the adsorption–desorption processes on a line [19]. Furthermore, a power law time dependence of the coverage followed by an exponential relaxation to equilibrium was suggested for the adsorption–desorption processes of  $k$ -mers on a one-dimensional lattice [21]. More recently, we have

carried out extensive simulations of the deposition processes for  $k$ -mers in the presence of desorption or/and diffusional relaxation on a one-dimensional lattice [22]. For the reversible deposition of  $k$ -mers, we have found that after the initial ‘jamming’, a stretched exponential growth of the coverage  $\theta(t)$  towards the equilibrium state value  $\theta_{\text{eq}}$  occurs, i.e.,  $\theta_{\text{eq}} - \theta(t) \propto \exp[-(t/\tau)^\beta]$ . The characteristic timescale  $\tau$  was found to decrease with the desorption probability  $P_{\text{des}}$  according to a power law,  $\tau \propto P_{\text{des}}^{-\gamma}$ , with the same exponent  $\gamma = 1.22 \pm 0.04$  for all  $k$ -mers.

Adsorption processes with diffusional relaxation lead to a fully covered lattice in the one-dimensional case and to the formation of large clusters of covered sites in the two-dimensional case. For these processes most authors propose a power law time dependence of the coverage in the late stages of deposition [22]–[24]. When adsorption, desorption and diffusion occur simultaneously, the system evolves to the equilibrium state. For one-component adsorption it has been shown [22, 25] that the presence of diffusion in the reversible case hastens the process, but the equilibrium coverage depends only on the desorption/adsorption probability ratio.

In some experimental situations, adsorbed particles such as colloidal ones and bioparticles are not monodisperse. Their size distributions may spread over several decades. The effect of size polydispersity on the growth of deposition structures was mainly studied to obtain their jamming limits and their late-time kinetics, which were different from those for the monodisperse case. The role of polydispersity in the irreversible deposition has been studied numerically and analytically. Numerical studies include the irreversible deposition of binary mixtures [26]–[29], and polydisperse mixtures of particles obeying uniform, Gaussian, and power law size distributions [9, 28, 30, 31]. Analytical studies were restricted to binary mixtures of particles with very large size differences [32]–[34], power law size distributions [31, 35], or general continuous size distributions [36]. The reversible RSA of binary mixtures of extended objects on a triangular lattice is discussed in [37]. The results of the numerical simulations indicate that the coverage kinetics for a mixture strongly depends on the symmetry properties of the component shapes.

In this work we present the results of extensive numerical simulations of generalized random sequential adsorption of mixtures containing various numbers of components of various lengths on a 1D lattice. The kinetics of the deposition process is studied for the irreversible case, for the adsorption–desorption processes and for the case where all three processes, i.e., adsorption, desorption and diffusion, are present simultaneously. Results for the irreversible deposition of mixtures are presented in section 2 and the influence of desorption and diffusion is discussed in section 3. Section 4 contains some additional comments and final remarks.

## 2. Random sequential adsorption of polydisperse mixtures

In the case of irreversible deposition, the dependence of the deposition kinetics on the number of components in the mixture and on the length of the depositing objects is investigated. The results are given for the whole mixture as well as for the individual components. An  $n$ -component mixture contains  $k$ -mers covering  $k = 2, 3, \dots, n+1$  lattice sites.

The Monte Carlo simulations are performed on a one-dimensional lattice of size  $L = 10^5$  with a periodic boundary condition. At each Monte Carlo step one of the  $n$

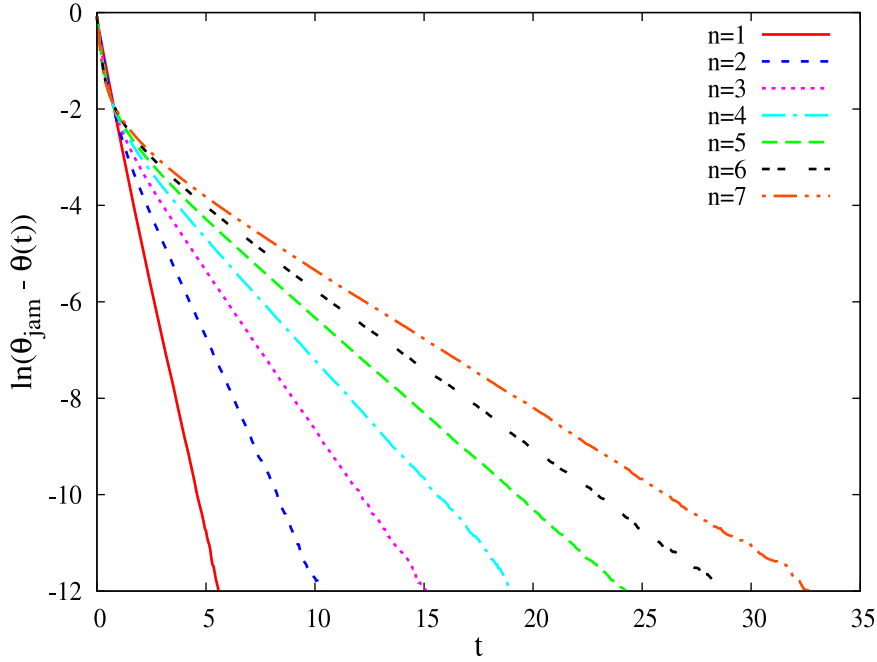


**Figure 1.** Plots of  $\ln[\theta_{\text{jam}} - \theta(t)]$  versus  $t$  for dimers ( $n = 1$ ), and for the six polydisperse mixtures with  $n = 2, \dots, 7$  components.

mixture components is chosen at random and one lattice site is selected at random. Then we try to deposit the  $k$ -mer with the beginning at the selected site, i.e., we search to find whether  $k$  consecutive sites are unoccupied. If so, we place the object. If not, the attempt is abandoned. Then a new depositing object from the mixture and a new site are selected at random, and so on. The jamming limit of the mixture  $\theta_{\text{jam}}$  is reached when none of the objects can be placed in any position on the lattice. The time is counted via the number of deposition attempts and scaled by the total number of lattice sites. The data are averaged over 1000 independent runs for each mixture.

The kinetics of the irreversible deposition of mixtures is illustrated in figure 1 where the plots of  $\ln[\theta_{\text{jam}} - \theta(t)]$  versus  $t$  are given for the six mixtures of  $k$ -mers made up of  $n = 2, \dots, 7$  components. In figure 2 the plots of such time dependences are shown for all the components making up a five-component mixture of  $k$ -mers ( $k = 2, \dots, 6$ ). It can be seen that for the late stages of the deposition process these plots are straight lines not only for the mixtures, but also for each of the components. This means that the exponential temporal evolution (1.1) of the coverage  $\theta(t)$  is valid both for the mixture and for the components making up the mixture. The values of the parameter  $\sigma$  are determined from the slopes of these lines. Parameter  $\sigma$  determines how fast the lattice is filled up to the jamming coverage  $\theta_{\text{jam}}$ . The parameter  $\sigma$  grows linearly with the number of components in the mixture, as shown in figure 3. The values of the relaxation times  $\sigma$  for the  $k$ -mers  $k = 2, \dots, 11$ , making up a ten-component mixture, are given in figure 4. The relaxation time  $\sigma$  decreases rapidly with the length of the components making up the mixture, so the late-time kinetics of the deposition is determined mostly by the smallest objects in the mixture. The reasons for these results are intuitively clear. Every occupation by

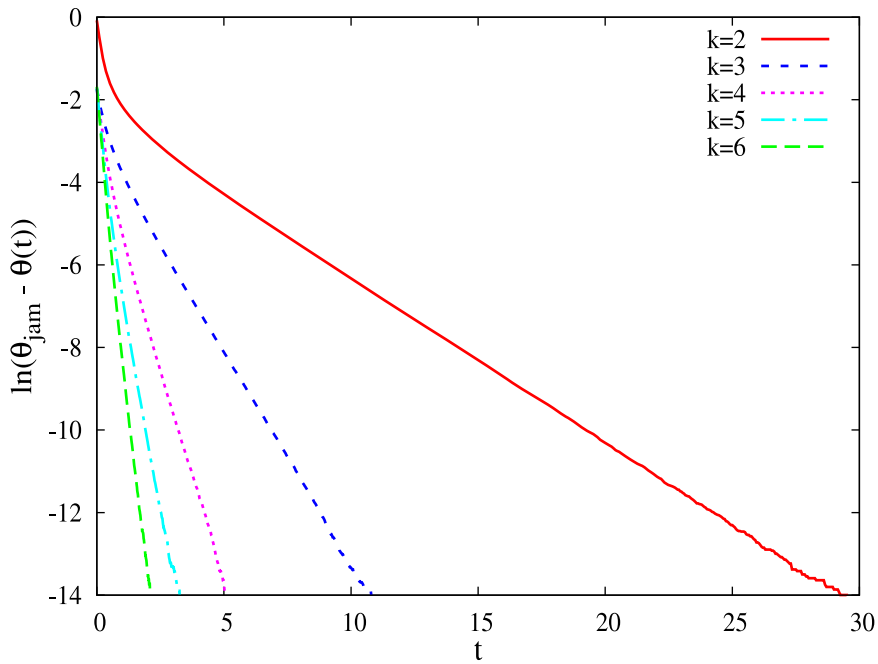


**Figure 2.** Plots of  $\ln[\theta_{\text{jam}} - \theta(t)]$  versus  $t$  for the components making up the five-component mixture of  $k$ -mers ( $k = 2, \dots, 6$ ).

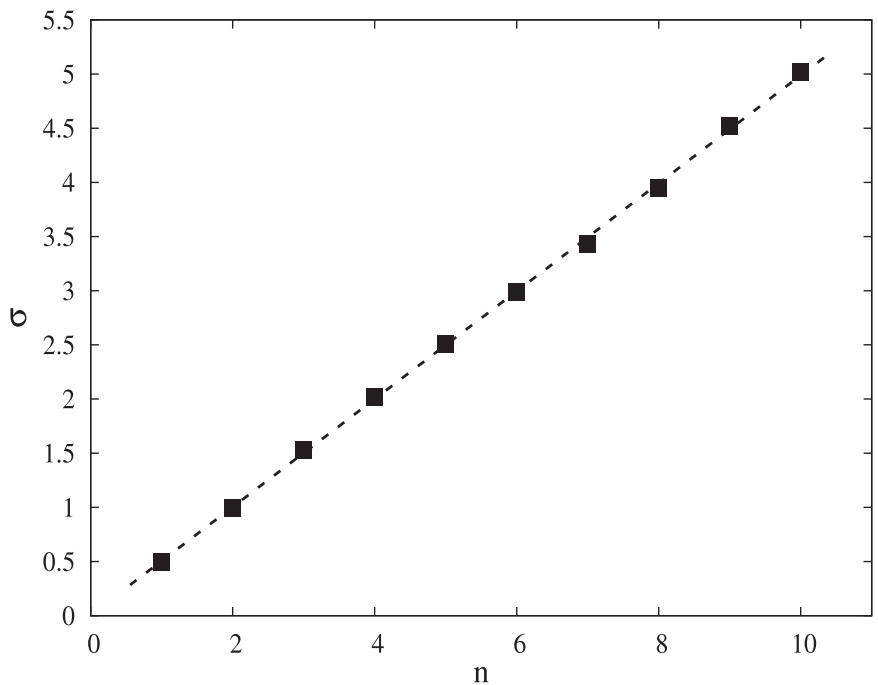


**Figure 3.** Dependence of the parameter  $\sigma$  (equation (1.1)) on the number of components in the mixture. The number of components is always increased by adding a  $k$ -mer of a greater size. The straight line with the slope  $\approx 1/2$  is the best linear fit through the data points.

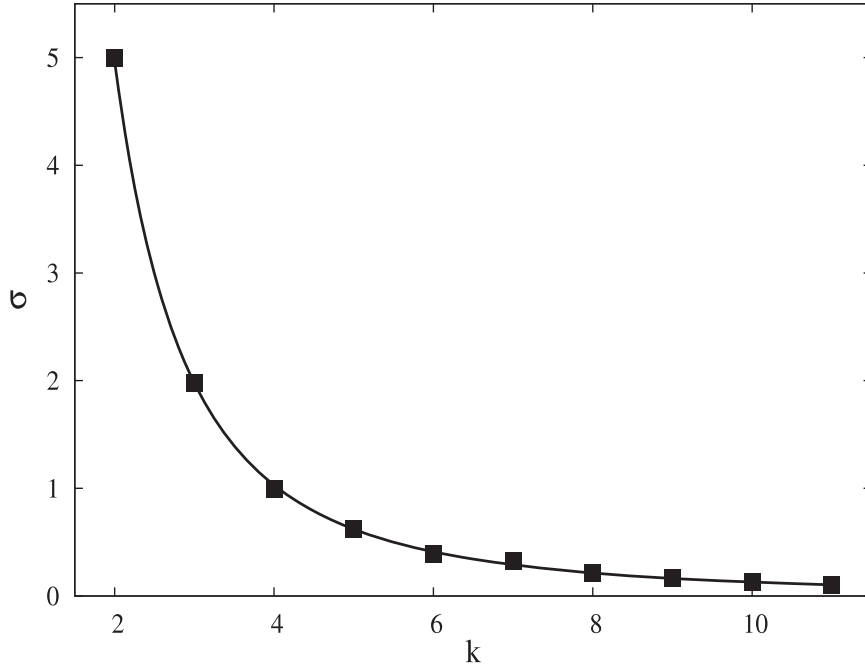
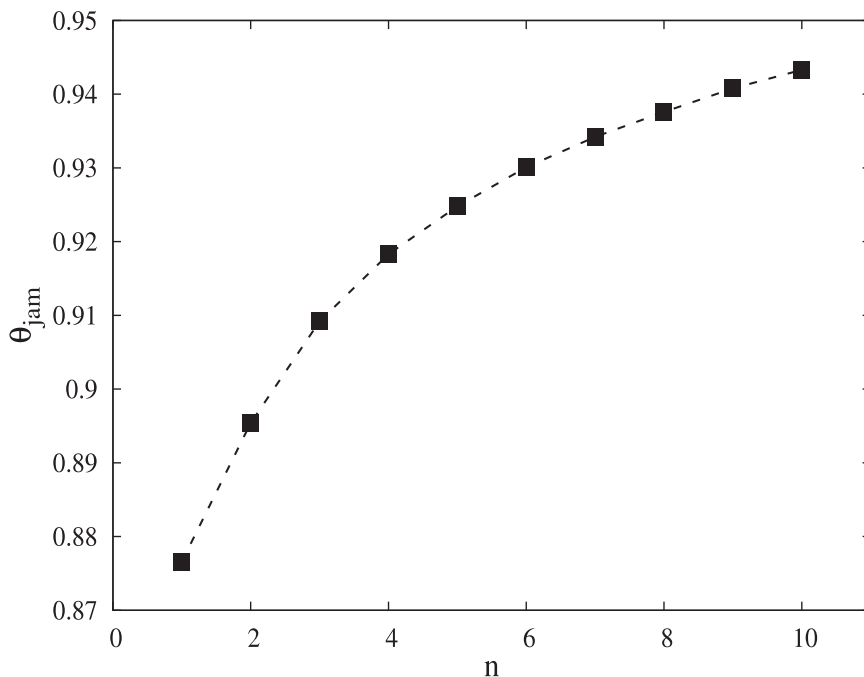


**Figure 4.** Dependence of the parameter  $\sigma$  (equation (1.1)) on  $k$  for the ten-component mixture of  $k$ -mers. The solid line represents the power law fit of the form  $\sigma = A k^{-\gamma}$ , with  $A = 23.92$  and  $\gamma = 2.269$ .

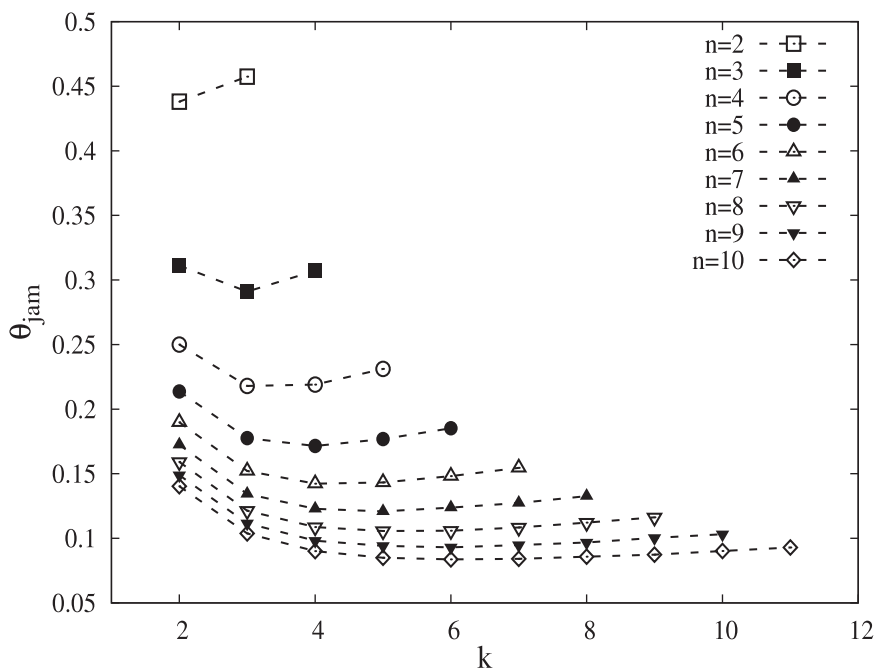
the smaller object creates an exclusion zone for further adsorption of larger objects. At large times, adsorption events take place on small domains of unoccupied sites, and in the competition between two objects of different numbers of segments the smaller object wins.

Figure 5 shows that the total jamming coverage  $\theta_{\text{jam}}$  increases with the number of components  $n$  in the mixture, despite the fact that the number of components is always increased by adding a  $k$ -mer of a greater length. Arbitrary mixtures thus cover the lattice more efficiently than either of the components. Partial jamming coverages are given in figure 6 for various mixtures starting from the two-component mixture of dimers and trimers and going to the ten-component mixture of  $k$ -mers ( $k = 2, 3, \dots, 11$ ). For the two-component mixture the partial jamming coverage of dimers is slightly smaller than that of trimers. In other mixtures, partial jamming coverage decreases with  $k$  for small  $k$ , reaches a minimum, and increases for sufficiently large  $k$ -mers. This minimum is shifted towards longer  $k$ -mers for greater number of components in the mixture. During the initial RSA regime adsorption events may be considered to take place on large regions of unoccupied lattice at a rate independent of the object size. When the lattice is partially filled with randomly distributed line segments of various lengths, it is much easier to add shorter objects than longer ones at random. Namely, with the growth of the coverage, the adsorption of longer  $k$ -mers is suppressed. At large times the number fraction of adsorbed  $k$ -mers in the mixture always decreases with  $k$ , as a consequence of the geometric exclusion effects. Nevertheless, for sufficiently large  $k$ -mers, the partial jamming coverage can increase with  $k$  due to the greater number of sites covered by a single  $k$ -mer.

Generalized random sequential adsorption of polydisperse mixtures on a one-dimensional lattice



**Figure 5.** Dependence of the total jamming coverage  $\theta_{\text{jam}}$  on the number of components in the mixture. The number of components  $n$  is always increased by adding objects of a greater size. The dashed line is a guide to the eyes.



**Figure 6.** Partial jamming coverages  $\theta_{\text{jam}}$  for the  $k$ -mers making up various  $n$ -component mixtures. The curves from top to bottom correspond to increasing values of  $n = 2, \dots, 10$ . The dashed lines are a guide to the eyes.



### 3. Adsorption, desorption and diffusion of mixtures

In this section we present the numerical studies of the effects of desorption and diffusion on deposition of mixtures in 1D. We investigate the role that the mixture composition plays in the time evolution of the coverage  $\theta(t)$  in the whole post-jamming time range. We carried out a detailed analysis of the contribution to the densification kinetics coming from each mixture component.

The Monte Carlo simulations of adsorption–desorption processes and processes where adsorption, desorption and diffusion are simultaneously present are performed on a one-dimensional lattice of size  $L = 10^5$ . The mixtures are made up of  $k$ -mers of various lengths. The time is rescaled to the adsorption process, because the number of adsorption attempts per unit of time is the quantity controlled in the experiments. The data are averaged over 100 independent runs for each of the processes investigated and for each combination of  $k$ -mers.

In the case of adsorption–desorption processes the kinetics is governed by the ratio of desorption to adsorption probability. At each Monte Carlo step adsorption is attempted with probability  $P_a$  and desorption with probability  $P_{des}$ . Since we are interested in the ratio  $P_{des}/P_a$ , in order to save computer time, it is convenient to take the adsorption probability to be  $P_a = 1$ . The algorithm for adsorption of a randomly chosen component of the mixture onto the lattice was already described in detail in the previous section. Each adsorption attempt is followed by a desorption attempt with probability  $P_{des}$ . The desorption process is started by choosing a lattice site at random. If this selected site is unoccupied, the desorption step fails and the process is continued by choosing a new site for an adsorption attempt. On the other hand, if a beginning of a deposited  $k$ -mer is at the selected site, the object is removed from the lattice.

When adsorption, desorption and diffusion are present simultaneously, the kinetics of the process is determined by the ratios of desorption/adsorption and diffusion/adsorption probabilities. Adsorption, desorption, and diffusion attempts are statistically independent and they are performed sequentially with probabilities  $P_a = 1$ ,  $P_{des}$ , and  $P_{dif}$ , respectively. Algorithms that describe the adsorption and desorption processes in our model have already been explained. If the attempted process is diffusion and if there is a beginning of a deposited object at the randomly selected site, we choose one of the two possible directions at random and try to move the  $k$ -mer by a lattice constant in that direction. The object is moved if it does not overlap with any of the deposited objects. If it does, the attempt is abandoned.

In order to gain a better insight into the complex kinetics of the adsorption–desorption processes of polydisperse mixtures it is useful to analyze in particular the process for the two-component mixtures. The simulations of adsorption–desorption processes were performed for various mixtures  $(k_1) + (k_2)$  of  $k$ -mers, such as  $(2) + (4)$ ,  $(2) + (6)$ ,  $(2) + (8)$ ,  $(2) + (10)$ ,  $(4) + (10)$ ,  $(6) + (10)$ , and  $(8) + (10)$ , and for various, relatively low, values of the desorption probability  $P_{des} = 0.001, 0.002, 0.005, 0.01, 0.02$ . The temporal evolutions of the total coverages for the reversible RSA of mixtures  $(2) + (4)$  and  $(8) + (10)$  are shown in figure 7. Also included in figure 7 are the time dependences of the partial coverages for each mixture component. Furthermore, the insets show the behaviors of the total and partial coverages in the early stages of the deposition process. The simulations were carried out with the desorption probability  $P_{des} = 0.005$ . As far as the partial coverages are

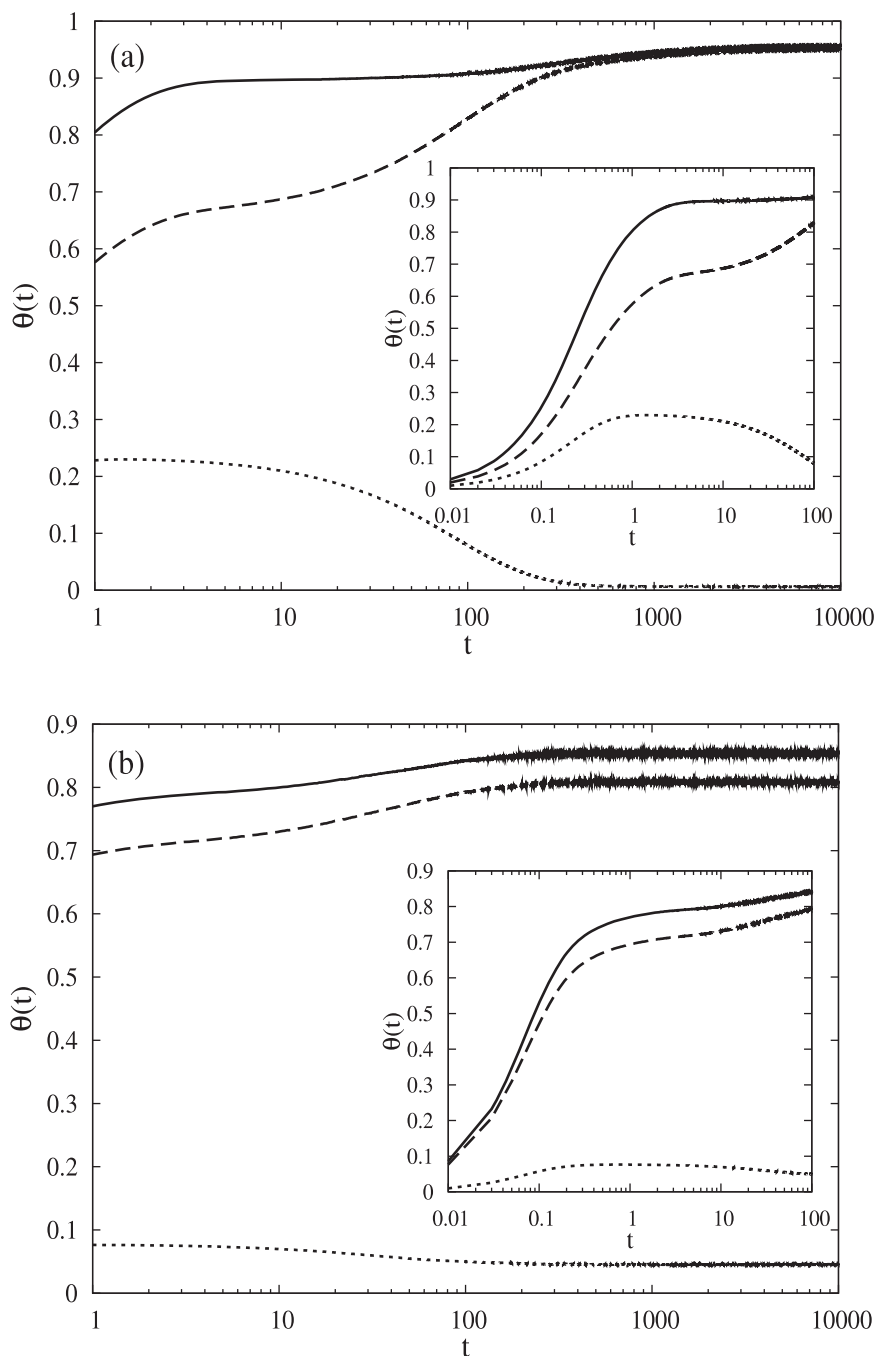


**Figure 7.** Shown here is the time dependence of the total coverage fraction  $\theta(t)$  for mixtures (a) (2) + (4) and (b) (8) + (10), together with the time dependences of the partial coverages of the components making up the mixture. All the results are for  $P_{\text{des}} = 0.005$ . The insets show the time evolution of the total and the partial coverages in the early stage of the deposition process. The solid lines represent the temporal behavior of the total coverage fraction. The dashed and dotted lines give the partial coverage fractions versus time  $t$  of the component  $k$ -mers: (2), (8)—dashed line, and (4), (10)—dotted line.

concerned, from figure 7 we can see that the coverage of a shorter object is a monotonically increasing function of time and has the same general features as the total coverage of the mixture. On the other hand, the partial coverage of the longer object is not monotonic in time. When the total coverage approaches the jamming limit, the partial coverage of the longer  $k$ -mer reaches a broad maximum (see the insets in figure 7). This is followed by a slow relaxation to the smaller equilibrium state value for the partial coverage of the longer component. The contribution of the longer  $k$ -mer to the total coverage fraction does not vanish for large times, but it becomes negligible. Hence, the dynamics of a mixture close to the equilibrium state limit is governed by the dynamics of the shorter  $k$ -mer. The equilibrium state values of the partial coverage depend on the desorption probability  $P_{\text{des}}$  and on the ratio of the object lengths,  $k_1/k_2$ .

In the initial stage, when the coverage fraction is small, the influence of desorption events is negligible compared with that of adsorption ones and the process displays an RSA-like behavior. At the beginning of the process, starting with an initially empty lattice, both mixture components adsorb with approximately equal rates and the coverage grows rapidly in time. With the growth of the coverage, adsorption of the longer  $k$ -mer is suppressed and the jamming of the mixture is reached by placing the shorter  $k$ -mers into the small empty regions. When a longer object desorbs, a shorter object has a greater number of possible places for adsorption into an empty region in the lattice, so the partial coverages of the longer  $k$ -mers decrease in time. At coverage close to the jamming limit  $\theta_{\text{jam}}$  for the irreversible case, the rare desorption events are followed by immediate readsorption. The growth of the coverage fraction of the mixture above  $\theta_{\text{jam}}$  requires rearrangement of the increasing number of objects in order to open a hole large enough for the insertion of an additional  $k$ -mer. Namely, when one badly sited object desorbs and two objects adsorb in the opened location, the number of  $k$ -mers is increased by 1. On the other hand, if two well sited objects desorb and a single object adsorbs in their stead, the number of  $k$ -mers is decreased by 1. These collective events are responsible for the growth of the coverage above  $\theta_{\text{jam}}$  [37]–[39]. We shall focus our attention on the kinetics in this post-jamming time range and on the approach to the equilibrium state.

We have found that above the jamming coverage, the time evolution of the total coverage of the mixture can be described by a stretched exponential function of the form

$$\theta(t) = \theta_{\text{eq}} - \Delta\theta \exp\left(-\left(t/\tau\right)^\beta\right). \quad (3.1)$$

The values of the equilibrium state coverage  $\theta_{\text{eq}}$ , the parameter  $\Delta\theta$  and the relaxation time  $\tau$  depend on the desorption probability  $P_{\text{des}}$  and on the mixture composition. In figure 8 the results of the simulations are shown together with fitting functions of the form (3.1) for three different mixtures. It should be noted that the value  $\theta_{\text{eq}}$  of the stretched exponential law is slightly higher than the final coverage fraction. This noticeable deviation is a consequence of the subsequent replacement of a small number of longer  $k$ -mers with shorter ones in the very late times of the deposition process. Strictly speaking, the stretched exponential law (3.1) holds in the intermediate relaxation regime until this replacement becomes the dominant mechanism for the final tuning of the equilibrium coverage. On the graphs in figure 8 vertical arrows indicate these moments.

An additional confirmation of the stretched exponential behavior of the coverage in the late stage of the adsorption–desorption processes of mixtures can be obtained by the

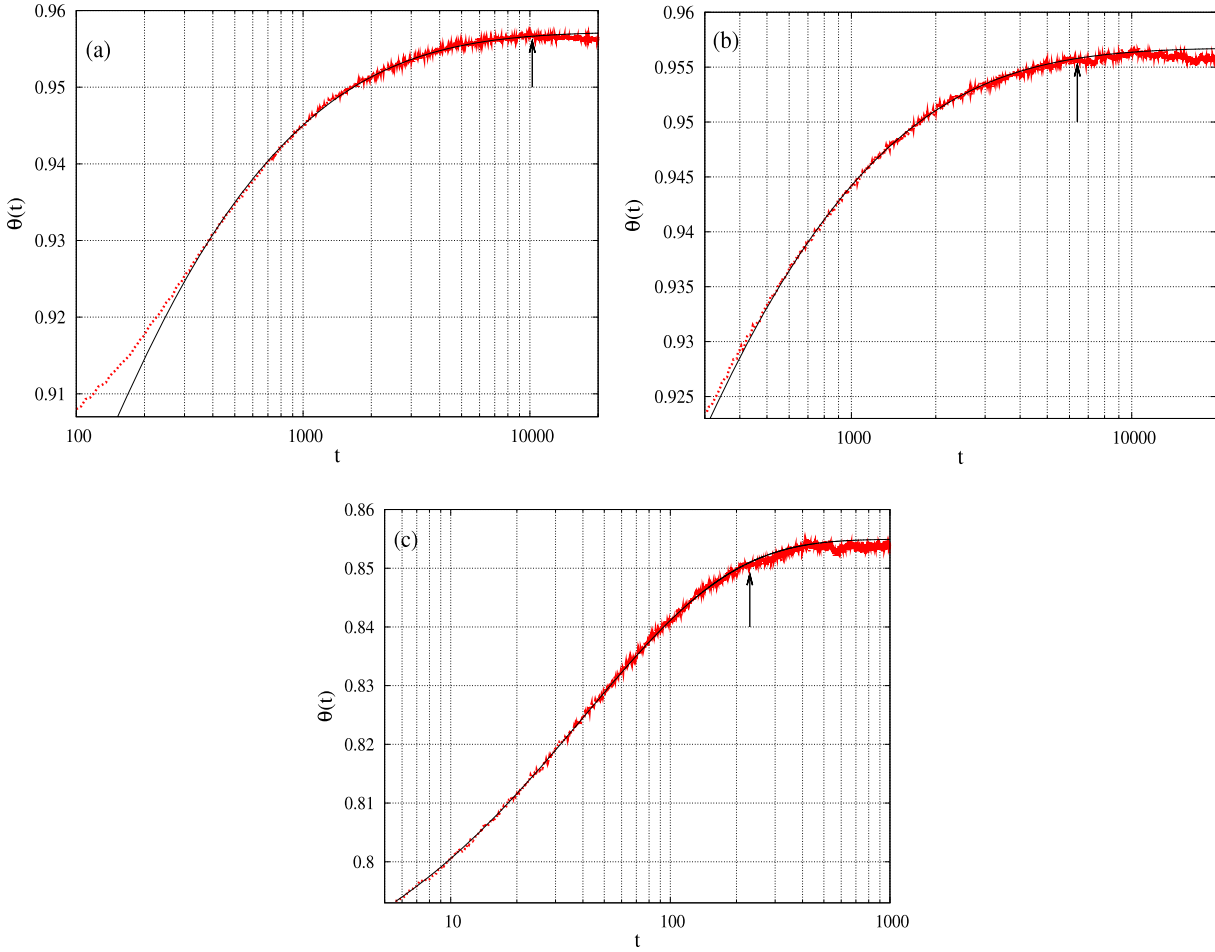


**Figure 8.** Temporal behavior of the coverage  $\theta(t)$  (red, dotted line) for the mixtures (a) (2)+(4), (b) (2)+(10), and (c) (8)+(10) in the case of reversible RSA. The continuous curves are the stretched exponential fits of equation (3.1). At the moments indicated by vertical arrows, the contribution of the replacements of longer objects with shorter ones to the kinetics of the process becomes dominant. All the results are for  $P_{\text{des}} = 0.005$ .

following analysis. Function (3.1) can be written as

$$\delta\theta(t) = \Delta\theta \exp\left(-\left(t/\tau\right)^\beta\right), \quad (3.2)$$

where  $\delta\theta = \theta_{\text{eq}} - \theta(t)$ . Differentiation of (3.2) gives

$$\frac{d\delta\theta(t)}{dt} = -\Delta\theta \exp\left(-\left(t/\tau\right)^\beta\right) \frac{\beta}{\tau} \left(\frac{t}{\tau}\right)^{\beta-1}, \quad (3.3)$$

i.e.,

$$-\frac{1}{\delta\theta(t)} \frac{d\delta\theta(t)}{dt} = \frac{\beta}{\tau^\beta} t^{\beta-1}. \quad (3.4)$$

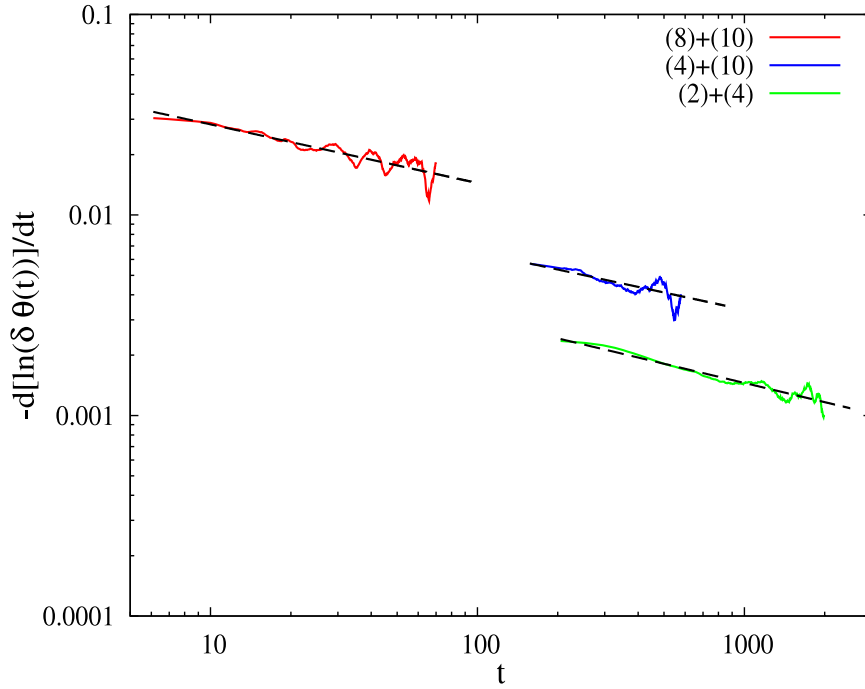


**Figure 9.** Test for the presence of the stretched exponential law (3.1) in the approach of the coverage  $\theta(t)$  to the steady state value for the mixtures: (8)+(10) (red, upper curve), (4) + (10) (blue, middle curve), and (2) + (4) (green, bottom curve). Straight line sections of the curves show where the law holds. The dashed lines are power law fits of equation (3.5). All the results are for  $P_{\text{des}} = 0.005$ .

From (3.4) it follows that

$$-\frac{d}{dt} [\ln(\delta\theta(t))] = \frac{\beta}{\tau^\beta} t^{\beta-1}, \quad (3.5)$$

which means that a double-logarithmic plot of the derivative of  $\ln[\delta\theta(t)]$  versus  $t$  is a straight line in the case of the stretched exponential function (3.1).

The double-logarithmic plots of the numerically calculated derivatives of  $\ln[\delta\theta(t)]$  for the data obtained by Monte Carlo simulations are straight lines for the coverages above the jamming coverage for all mixtures and for all values of the desorption probabilities. Such plots are shown in figure 9 for three different mixtures for the case of  $P_{\text{des}} = 0.005$ . This strongly suggests that the relaxation to the equilibrium state in the case of adsorption–desorption processes of mixtures is mainly governed by the stretched exponential law. Values of the fitting parameters  $\tau$  and  $\beta$  are determined from the slopes of these lines and the values of  $\Delta\theta$  are obtained by using the least-squares method for a given pair  $(\tau, \beta)$ . Note that the fitting parameters  $\tau$ ,  $\beta$  and  $\Delta\theta$  in the fitting functions shown in figure 8 are obtained as described above.

Simulations of the adsorption–desorption processes are also performed for the ten-component mixture made up of  $k$ -mers covering 2, 3, 4, ..., and 11 lattice sites. Results are obtained for various low desorption probabilities in the range from  $P_{\text{des}} = 0.0002$  to  $P_{\text{des}} = 0.002$ . The results for the time evolution of the partial and total coverages in the case of  $P_{\text{des}} = 0.002$  are given in figures 10(a) and (b), respectively. From figure 10(a) we

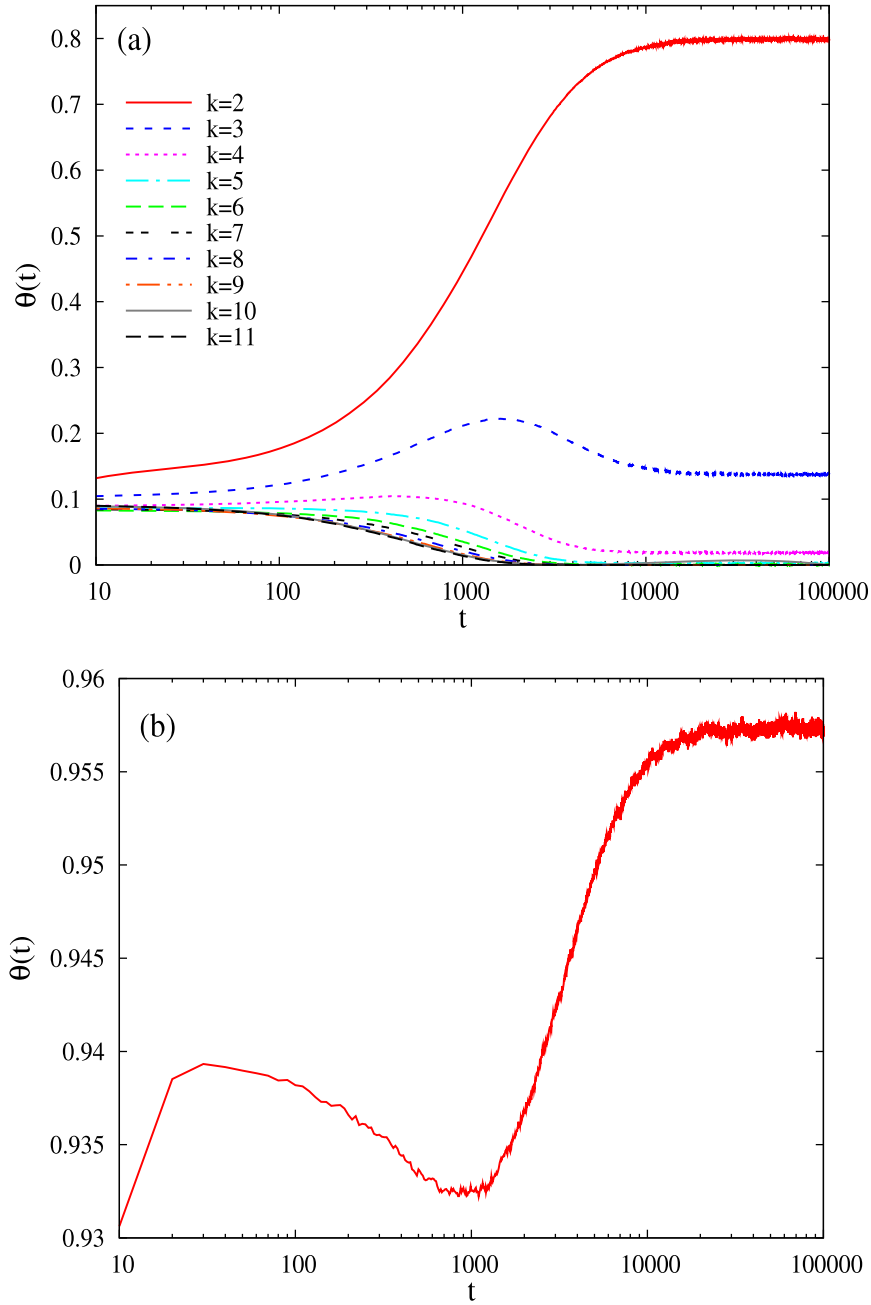


**Figure 10.** (a) Time dependences of the partial coverages  $\theta(t)$  for the ten-component mixture of  $k$ -mers ( $k = 2, 3, \dots, 11$ , from top to bottom). (b) Time dependence of the total coverage fraction  $\theta(t)$  for the same mixture. All the results are for  $P_{\text{des}} = 0.002$ .

can see that only the time dependence of the partial coverage of dimers is monotonically increasing. Partial coverage corresponding to any of the other components increases at the early times of the deposition process, reaches a maximum and decreases slowly to its equilibrium value afterward. Figure 10(b) shows that starting from an initially empty lattice, the total coverage increases and reaches a local maximum value first. Interestingly,

then the total coverage starts to decrease and reaches a wide minimum. In the final stage, it slowly relaxes to the equilibrium value via collective rearrangements. The initial phase consists of RSA of  $k$ -mers. After this initial filling of the lattice, adsorption becomes slower and desorption can no longer be ignored. Then, the change of the coverage is caused by a long sequence of desorption–adsorption events in which a  $k$ -mer detaches from the lattice and the gap that is created is immediately filled by one or more new  $k$ -mers. In this late stage, RSA acts to preferentially adsorb the shorter  $k$ -mers. This is a consequence of the fact that unlike for the very long  $k$ -mers, many more possible places for deposition are allowed for short  $k$ -mers falling in the isolated empty location. Therefore, the partial coverages of longer objects decrease in time, causing the decrease of the total coverage until the collective effects take place. Fine-tuning of the incoming and outgoing flux of each component occurs during this stage. In the final regime, the coverage of the mixture increases due to the increase of the number of deposited dimers.

Above the jamming limit, the time evolution of the total coverage  $\theta(t)$  for the ten-component mixture can also be well described by the stretched exponential law (3.1). Examples of such fits are shown in figure 11 together with the results of the simulations for three different desorption probabilities,  $P_{\text{des}} = 0.0004, 0.0008, 0.001$ . The reasons for the deviations between the results of the simulations and the corresponding fitting functions, visible in the final phase of the process, are similar to those for the case of the two-component mixture. These deviations increase gradually with the turning on of various combinations of replacements of longer objects with shorter ones.

The dependence of the total equilibrium coverage  $\theta_{\text{eq}}$  on the desorption probability  $P_{\text{des}}$  is shown in figure 12 for the ten-component mixture. The equilibrium coverage  $\theta_{\text{eq}}$  is found to decrease with the desorption probability  $P_{\text{des}}$  according to an exponential law:

$$\theta_{\text{eq}} = \theta_0 + \theta_1 e^{-P_{\text{des}}/P_0}, \quad (3.6)$$

with parameters  $\theta_0 = 0.949$ ,  $\theta_1 = 0.042$ , and  $P_0 = 0.0013$ .

The values of the fitting parameter  $\tau$  for the various desorption probabilities in the range  $P_{\text{des}} \in [10^{-4}, 10^{-3}]$  are shown in figure 13 on a log–log scale. As for the pure depositing objects, the dynamics of the reversible RSA of polydisperse mixtures gets drastically slower when the desorption probability decreases. For the ten-component mixture the values of the fitting parameter  $\beta$  are determined from the slopes of  $\ln(\delta\theta(t))$  lines (equation (3.5)). At low values of the desorption probability  $P_{\text{des}}$  in the range of  $10^{-4}$ – $10^{-3}$ ,  $\beta$  is in the range of 0.33–0.55.

Finally, we consider the general case of the reversible RSA of polydisperse mixtures on the 1D lattice in the presence of diffusion. Adsorption–desorption processes with diffusional relaxation are reversible and after a long enough time the system reaches an equilibrium state. This is illustrated in figure 14 where the time dependence of the total coverage  $\theta(t)$  in the case of reversible deposition of the ten-component mixture is shown for various values of the diffusion probability,  $P_{\text{dif}} = 0.2, 0.4, 0.6, 0.8, 1.0$ . Also included in figure 14 is the temporal evolution of the total coverage  $\theta(t)$  for the same mixture, but without diffusion. There is a significant difference in time behavior of the coverage with diffusion and that without. As in the case of a pure adsorption–desorption process, the early stage of the process is dominated by adsorption. With the growth of the coverage, desorption and diffusion events take place and the coverage decreases due to the replacement of longer objects by shorter ones. When the diffusion



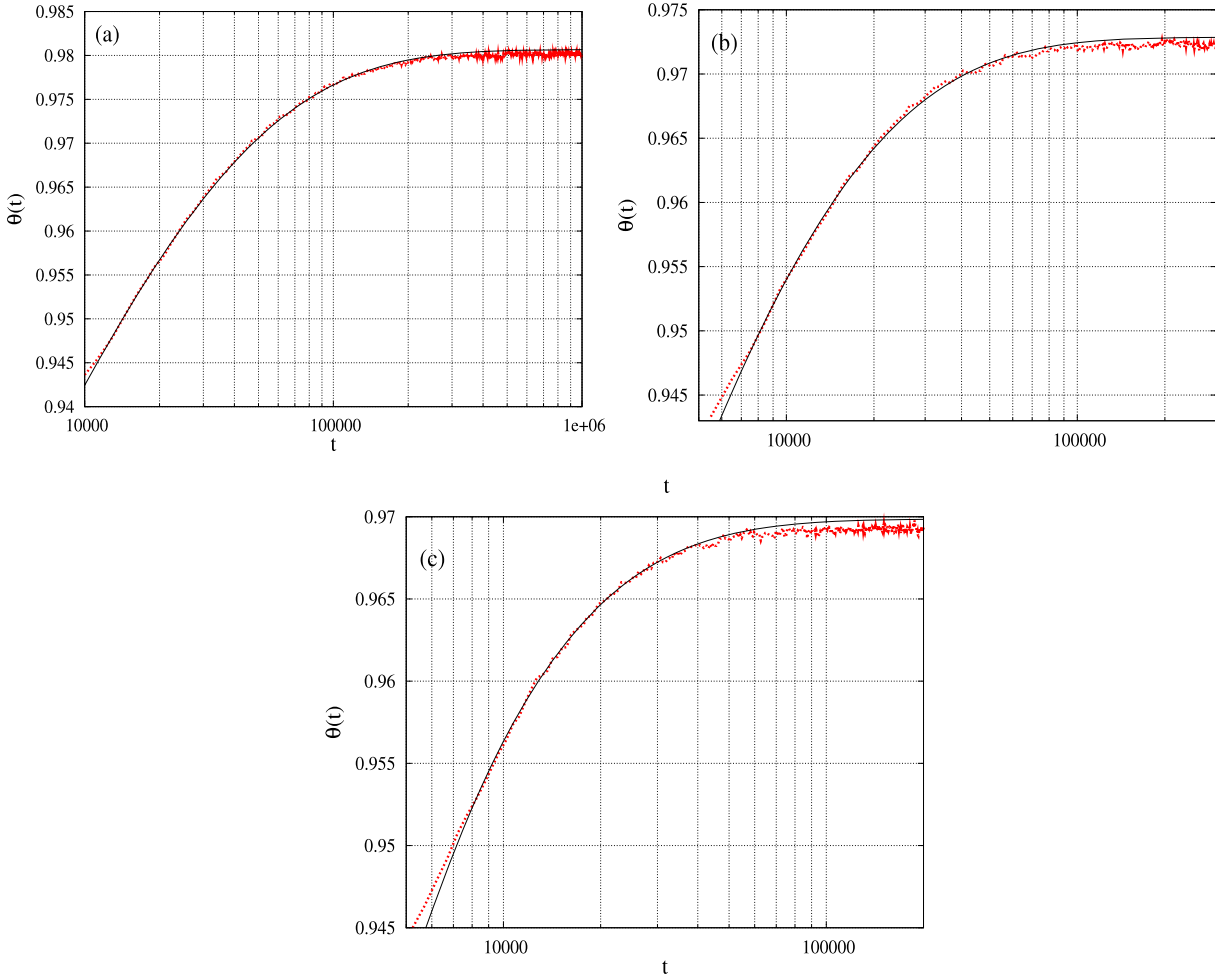


**Figure 11.** Temporal behavior of the coverage  $\theta(t)$  (red, dotted line) for the ten-component mixture of  $k$ -mers ( $k = 2, 3, \dots, 11$ ) for the cases of (a)  $P_{\text{des}} = 0.0004$ , (b)  $P_{\text{des}} = 0.0008$ , and (c)  $P_{\text{des}} = 0.001$ . The continuous curves are the stretched exponential fits of equation (3.1).

of the deposited objects is not allowed, the coverage increases again due to the collective events. In the presence of diffusion, with diffusional probabilities significantly greater than the desorption probability, the quick rearrangement of deposited objects disallows the subsequent increase of the coverage and the equilibrium coverage is slightly lower than in the case without diffusion. This is in contrast with the results obtained for the one-component two-dimensional case [25] where the equilibrium coverage is not affected by the presence of diffusion.

#### 4. Concluding remarks

We have investigated numerically the kinetics of deposition process of mixtures of  $k$ -mers on a 1D lattice in the presence of desorption and diffusion of depositing objects. We focused on the time evolution of the coverage  $\theta(t)$  in the whole post-jamming time range ( $\theta(t) > \theta_{\text{jam}}$ ). A systematic approach is made by examining a wide variety of  $k$ -mers and



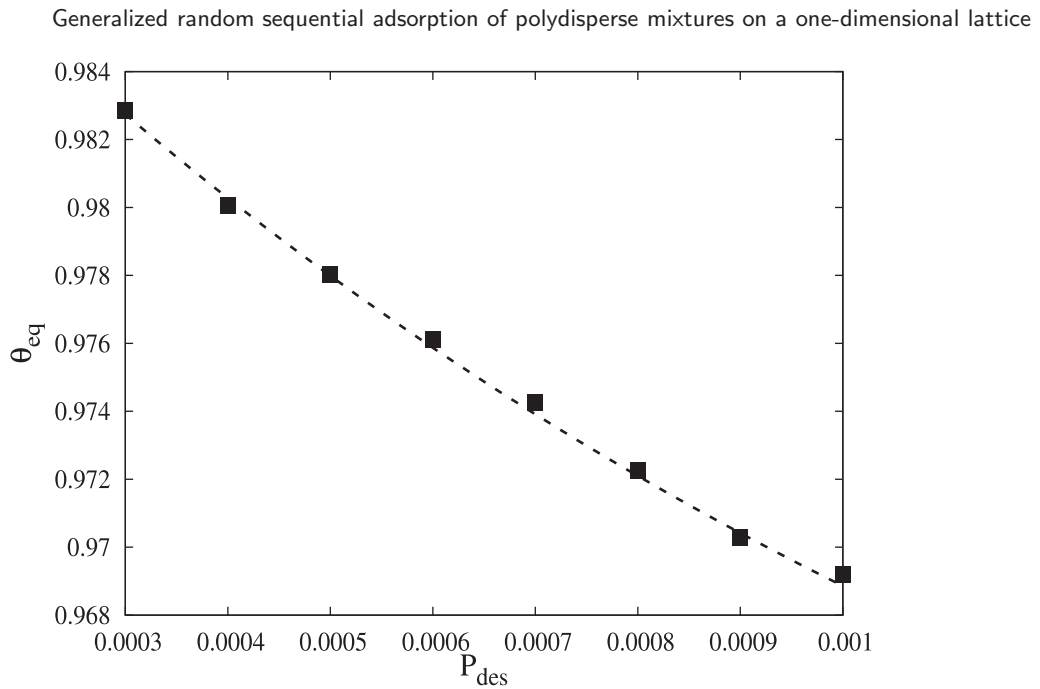


**Figure 12.** Plot of the total equilibrium coverage  $\theta_{\text{eq}}$  against the desorption probability  $P_{\text{des}}$  for the ten-component mixture of  $k$ -mers ( $k = 2, 3, \dots, 11$ ). The dashed line is the exponential fit of equation (3.6).

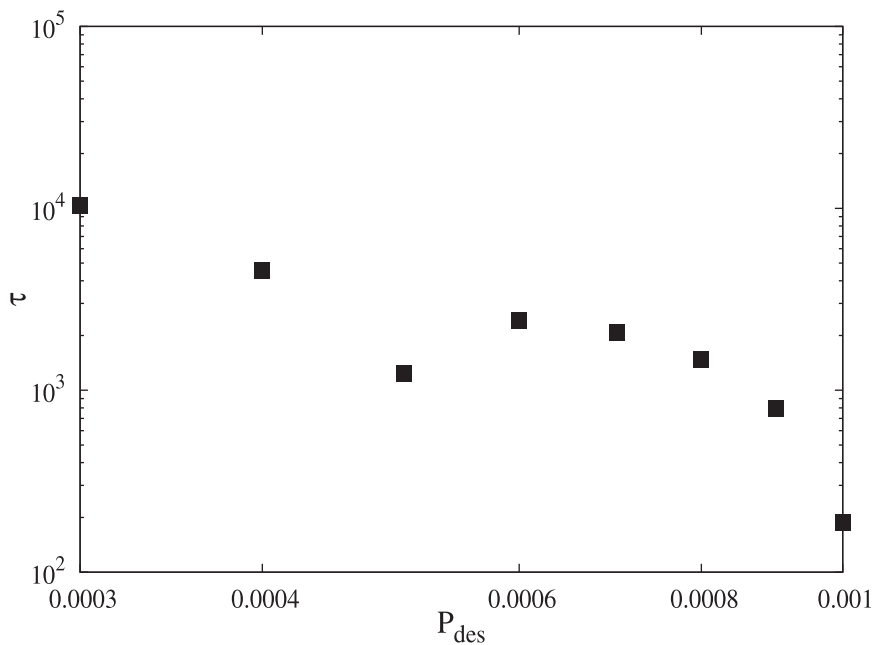


**Figure 13.** Dependence of the parameter  $\tau$  on the desorption probability  $P_{\text{des}}$  for the ten-component mixture of  $k$ -mers.

their mixtures. In the case of the irreversible deposition, special attention is paid to the dependence of the densification kinetics on the number of components in the polydisperse mixture. The number of components is gradually increased by adding a line segment

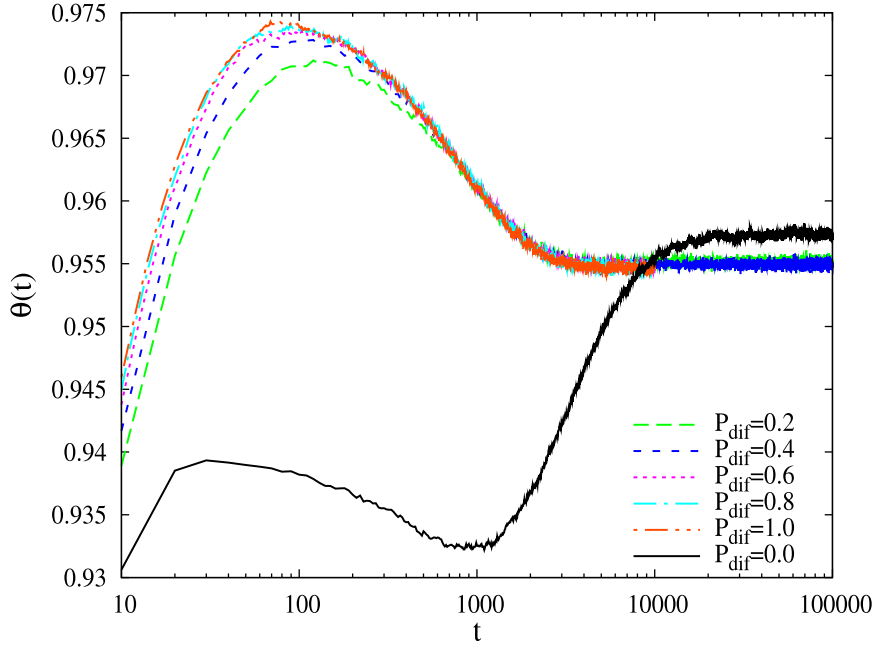


**Figure 14.** Temporal behavior of the total coverage  $\theta(t)$  for the ten-component mixture of  $k$ -mers ( $k = 2, 3, \dots, 11$ ) in the case of  $P_{\text{des}} = 0.002$  and for various diffusion probabilities,  $P_{\text{dif}} = 0.2, 0.4, 0.6, 0.8, 1.0$ . The solid (black) line shows the time dependence of the total coverage  $\theta(t)$  for the same value of  $P_{\text{des}}$ , but without diffusion.

of a greater length. We have performed a detailed analysis of the contribution to the densification kinetics coming from each mixture component.

It was shown that the exponential behavior (equation (1.1)) describes the approach to the jamming limit excellently in the case of irreversible deposition of polydisperse mixtures of  $k$ -mers. The relaxation time  $\sigma$  grows linearly with the number of components in the mixture. Components also reach their contribution to the jamming limit exponentially and the corresponding relaxation times  $\sigma$  decrease very rapidly with the size of the  $k$ -mers. It was found that the total jamming coverage increases with the number of components. The jamming coverage for a mixture is always greater than either of the jamming coverages of the components making up the mixture.

We have also presented the numerical results for the reversible RSA both for binary and for multicomponent mixtures of  $k$ -mers. It was shown that the growth of the coverage  $\theta(t)$  above the jamming limit  $\theta_{\text{jam}}$  to the equilibrium coverage  $\theta_{\text{eq}}$  occurs via the stretched exponential law (3.1), for all mixtures and for all values of the desorption probability  $P_{\text{des}}$ . The stretched exponential law (3.1) holds in the intermediate relaxation regime until the replacement of longer objects with shorter ones becomes the dominant mechanism that governs the late stage of the process. The characteristic timescale  $\tau$  was found to decrease with the desorption probability. We have also discussed the significance of collective events for governing the time coverage behavior of component  $k$ -mers. In comparison to the monodisperse case, the analysis is more complex for mixtures, because of the large variety of spatial arrangements corresponding to events that involve two and more line segments

of various lengths. With the example of a ten-component mixture, it was demonstrated that the coverage kinetics of a mixture has a richer behavior in comparison to that of the reversible deposition of pure lattice objects. In the presence of desorption, the total coverage of a polydisperse mixture is not always monotonic in time (figure 10) as a result of the interplay between the incoming and the outgoing flux of each mixture component.

When adsorption, desorption and diffusion perform simultaneously, the system always reaches an equilibrium state. In the case of a single-component deposition process, the equilibrium coverage  $\theta_{\text{eq}}$  depends only on the desorption/adsorption probability ratio [22, 25, 40] and the presence of diffusion only hastens the approach to the equilibrium state. However, in the case of polydisperse mixtures there is a significant difference in temporal evolution for coverage with diffusion and that without. Diffusional rearrangements of line segments of various lengths enable the growth of the coverage in the late stage of the process. The coverage decreases due to the replacement of longer deposited objects by shorter ones and the equilibrium coverage in the presence of diffusion is lower than for the pure adsorption–desorption processes.

## Acknowledgments

This work was supported by the Ministry of Science of the Republic of Serbia, under Grant No. 141035. The simulations were performed in the ‘Center for Meteorology and Environmental Prediction—Advanced Computing Laboratory’.

## References

- [1] Flory P J, 1939 *J. Am. Chem. Soc.* **61** 1518
- [2] Evans J W, 1993 *Rev. Mod. Phys.* **65** 1281
- [3] Talbot J, Tarjus G, Van Tassel P R and Viot P, 2000 *Colloids Surf. A* **165** 287
- [4] Senger B, Voegel J C and Schaaf P, 2000 *Colloids Surf. A* **165** 255
- [5] Cadilhe A, Araújo N A M and Privman V, 2007 *J. Phys.: Condens. Matter* **19** 065124
- [6] Bartelt M C and Privman V, 1990 *J. Chem. Phys.* **93** 6820
- [7] Manna S S and Švrakić N M, 1991 *J. Phys. A: Math. Gen.* **24** L671
- [8] Budinski-Petković Lj and Kozmidis-Luburić U, 1997 *Phys. Rev. E* **56** 6904
- [9] Budinski-Petković Lj, Vrhovac S B and Lončarević I, 2008 *Phys. Rev. E* **78** 061603
- [10] Ramsden J J, Bachmanova G I and Archakov A I, 1994 *Phys. Rev. E* **50** 5072
- [11] Talbot J, Tarjus G and Viot P, 2000 *Phys. Rev. E* **61** 5429
- [12] Budinski-Petković Lj and Vrhovac S B, 2005 *Eur. Phys. J. E* **16** 89
- [13] Frey E and Vilfan A, 2002 *Chem. Phys.* **284** 287
- [14] Knight J B, Fandrich C G, Lau C N, Jaeger H M and Nagel S R, 1995 *Phys. Rev. E* **51** 3957
- [15] Philippe P and Bideau D, 2002 *Europhys. Lett.* **60** 677
- [16] Ribière P, Richard P, Bideau D and Delannay R, 2005 *Eur. Phys. J. E* **16** 415
- [17] Budinski-Petković Lj, Petković M, Jakšić Z M and Vrhovac S B, 2005 *Phys. Rev. E* **72** 046118
- [18] Josserand C, Tkachenko A, Mueth D M and Jaeger H M, 2000 *Phys. Rev. Lett.* **85** 3632
- [19] Krapivsky P L and Ben-Naim E, 1994 *J. Chem. Phys.* **100** 6778
- [20] Budinski-Petković Lj and Kozmidis-Luburić U, 2001 *Physica A* **301** 174
- [21] Ranjith P and Marko J F, 2006 *Phys. Rev. E* **74** 041602
- [22] Lončarević I, Budinski-Petković Lj, Vrhovac S B and Belić A, 2009 *Phys. Rev. E* **80** 021115
- [23] Fusco C, Gallo P, Petri A and Rovere M, 2001 *J. Chem. Phys.* **114** 7563
- [24] Lee J W and Hong B H, 2003 *J. Chem. Phys.* **119** 533
- [25] Budinski-Petković Lj and Tošić T, 2003 *Physica A* **329** 350
- [26] Bonnier B, Leroyer Y and Pommiers E, 1992 *J. Physique I* **2** 379
- [27] Barker G C and Grimson M J, 1988 *Mol. Phys.* **63** 145
- [28] Meakin P and Jullien R, 1992 *Phys. Rev. A* **46** 2029
- [29] Lončarević I, Budinski-Petković Lj and Vrhovac S B, 2007 *Eur. Phys. J. E* **24** 19
- [30] Adamczyk Z, Siwek B, Zembala M and Weron P, 1997 *J. Colloid Interface Sci.* **185** 236

- [31] Brilliantov N V, Andrienko Y A, Krapivsky P L and Kurths J, 1996 *Phys. Rev. Lett.* **76** 4058
- [32] Talbot J and Schaaf P, 1989 *Phys. Rev. A* **40** 422
- [33] Bartelt M C and Privman V, 1991 *Phys. Rev. A* **44** R2227
- [34] Tarjus G and Talbot J, 1992 *Phys. Rev. A* **45** 4162
- [35] Krapivsky P L, 1992 *J. Stat. Phys.* **69** 135
- [36] Tarjus G and Talbot J, 1991 *J. Phys. A: Math. Gen.* **24** L931
- [37] Lončarević I, Budinski-Petković Lj and Vrhovac S B, 2007 *Phys. Rev. E* **76** 031104
- [38] Kolan A J, Nowak E R and Tkachenko A V, 1999 *Phys. Rev. E* **59** 3094
- [39] Ghaskadvi R S and Dennin M, 2000 *Phys. Rev. E* **61** 1232
- [40] de Mendonca J R G and de Oliveira M J, 1998 *J. Stat. Phys.* **92** 651